International Journal of Fatigue 99 (2017) 78–86

Contents lists available at ScienceDirect

International Journal of Fatigue

journal homepage: www.elsevier.com/locate/ijfatigue

Cyclic behavior and modeling of small fatigue cracks of a polycarbonate polymer

J.M. Hughes [a,*], M. Lugo [b], J.L. Bouvard [a,c], T. McIntyre [a], M.F. Horstemeyer [a,d]

[a] Center for Advanced Vehicular System, Mississippi State University, Starkville, MS 39759, USA
[b] Department of Mechanical Engineering, University of Texas of the Permian Basin, Odessa, TX 79762, USA
[c] MINES ParisTech, PSL-Research University, CEMEF – Centre de Mise en Forme des Matériaux, CNRS UMR 7635, CS 10207 rue Claude Daunesse, 06904 Sophia Antipolis Cedex, France
[d] Department of Mechanical Engineering, Mississippi State University, Starkville, MS 39759, USA

ARTICLE INFO

Article history:
Received 22 June 2016
Received in revised form 3 December 2016
Accepted 6 December 2016
Available online 8 December 2016

Keywords:
Polycarbonate
MultiStage Fatigue
Uncertainty

ABSTRACT

The fatigue behavior of a polycarbonate (PC) thermoplastic material was experimentally investigated and modeled using a MultiStage Fatigue (MSF) model that evaluates fatigue crack incubation, Microstructurally Small Crack (MSC) growth, and Long Crack (LC) growth. A set of fully reversed strain controlled tests were conducted, and an analysis of the fracture surfaces was performed using Scanning Electron Microscopy (SEM) in order to quantify the structure-property relationships for the MSF model. Fractography of the microstructure revealed that incompletely melted PC pellets were present in the polymer material that nucleated the cracks along with crazes generated on the surface. Crack lengths and fatigue crack growth rates for the MSC regime were measured from striation observations on the fracture surfaces. Discontinuous crack growth (DCG) cycles between fatigue striations, for the current iteration of the model, are accounted for by the MSF crack incubation regime. Finally, the microstructure sensitive MSF model was implemented using the observed fatigue crack growth measurements. In addition, a Monte Carlo (MC) Simple Random Sampling (SRS) routine was implemented to quantify the model uncertainty for crack growth.

1. Introduction

Polymers are used in many engineering applications such as aerospace structures, automotive parts, pressure vessels, and military equipment and vehicles. Currently, polymers are attracting much attention because the potential of lightening these mechanical structures. Like other engineering materials, polymers fail as a result of fatigue damage from the nucleation and growth of fatigue cracks. Therefore, an extensive use of polymeric materials requires a better understanding of its fatigue behavior.

Traditionally, fracture mechanics has been employed to characterize the cyclic behavior of polymers [11,8,9,27,24,25,13]. The study of fatigue crack propagation in polymers allows a detailed analysis of the fracture process. In addition, the study of fatigue using the fracture mechanics method allows for the separation of the initiation and crack propagation stages [11,9]. For crack propagation in thermoplastics two different processes have been identified, normal and retarded crack growth [14], with both being associated with craze evolution at the crack tip. In the analysis of the fracture surface for polymers there has been observed two types of marks [25], which are associated with the two types of crack propagation: continuous and discontinuous crack propagation [25]. Other factors that affect crack propagation have also been studied such as microstructure [16], blend composition and frequency [7], and the stress ratio and molecular weight [22].

It is generally accepted that fatigue life consists of two stages: crack initiation and crack growth or propagation [29,28,3]. The total number of cycles to initiate a crack is usually determined by the use of the strain-life method while crack growth to failure is determined by fracture mechanics [28]. Nonetheless, in design engineering applications, fracture mechanics is used to design against fatigue in polymers. This approach assumes the existence of a pre-crack and the crack propagation dominates the fatigue life of the component. Therefore, conventional design with polymers is only based on the long fatigue crack growth regime.

Although fracture mechanics provides a tool to characterize crack propagation, it characterizes only the growth of long cracks. It has been found that short cracks behave differently than long cracks [30,31,21]. Among the differences are crack growth rate

* Corresponding author.

http://dx.doi.org/10.1016/j.ijfatigue.2016.12.012
0142-1123/

and crack path. Crack growth rate shows inclusion size dependency when the crack size is comparable to microstructural features [29]. Additionally, it has been observed that small cracks usually initiate from defects found in the material [29,30].

In order to quantify the fatigue life associated with short fatigue cracks, the MultiStage Fatigue (MSF) model's microstructurally small crack (MSC) growth regime is considered. The MSF model was originally developed for an A356 aluminum alloy [19] and has since been expanded for use with various other aluminum alloys [12,32], magnesium [4,33], and an ABS copolymer [17]. Lugo et al. demonstrated that the MSF model framework was general enough to handle polymeric materials. Due to the possibility of discontinuous crack growth in polycarbonate, this model effectively only describes periods of crack extension; that is, the cycles between striations before craze breakdown are excluded for the current model iteration. Future extensions focusing on craze formation and breakdown will inevitably need to be added.

While investigations addressing the long crack growth behavior of polymers are abundant, fatigue studies on polymers that incorporate small crack behavior and microstructural features into cyclic models are virtually nonexistent. In this research the fatigue performance of a polycarbonate thermoplastic polymer was investigated. A set of fully reversed fatigue tests were conducted and an analysis of the fracture surfaces was performed using scanning electron microscopy (SEM). The objective was to investigate the use of microstructure-sensitive small fatigue crack growth model for use with thermoplastic materials.

2. Materials and experiments

The material in this investigation is a Makrolon grade, amorphous, glassy polycarbonate (PC) thermoplastic. This material was chosen due to its purported insensitivity to test frequency [9] in order to determine the effectiveness of the MSF model for capturing inclusion size dependency. Here, an inclusion is defined as being any pore, particle, or void that incubates a dominant small fatigue crack. The term void is used to differentiate pre-existing microstructural pores due to processing from those that may have been created due to induced stresses and strains and are typically much larger than the average pore size. Monotonic tensile and compression experiments were performed using an Instron 8850 load frame with an Instron 2630-110 extensometer to monitor axial strains. Flat dog-bone tensile specimens were made following ASTM D638-03 standard [1]. For compression tests, cylindrical specimens similar to those employed by [20] were used. A molypaste lubricant was used with the compression tests to minimize friction between the specimen and compression platens to reduce barreling.

Completely reversed, uniaxial fatigue experiments were conducted using an MTS 810 servo-hydraulic load frame with an MTS model 643.31F-25 axial extensometer for the strain control tests. Testing was conducted at strain amplitudes of 0.0065 to 0.02 and at frequencies of 1 and 10 Hz using a ramp wave. Cylindrical dog-bone shaped specimens were machined from the supplied plates on a CNC lathe to the dimensions shown in Fig. 1. Before testing, each specimen was progressively sanded and polished using 240, 800, 1200, and 2400 grit sandpaper to produce a smooth surface. The polished surface was inspected with an optical microscope to ensure that all machine marks perpendicular to the load direction were removed.

Fracture surfaces of the fatigued specimens were prepared for SEM observation. Specimens were glued to an aluminum base with a carbon-based epoxy and subsequently sputter coated for two minutes following a 12 h curing in a desiccator.

3. Results and discussion

3.1. Microstructure

Like other amorphous thermoplastic materials, PC is formed of long polymer chains that are randomly oriented and entangled. Unlike metals, thermoplastics like PC do not have definitive, quantifiable microstructure features. For the PC of this study, SEM analysis revealed the existence of inclusion particles in the form of partially melted pellets embedded in the amorphous matrix (Fig. 2). Conglomerations of these inclusions (Fig. 3) were observed near the free surface and at crack incubation sites, thus contributing to the generation of fatigue cracks.

3.2. Stress-strain behavior

The monotonic stress-strain curves of the PC thermoplastic polymer in tension and compression are given in Fig. 4. True stress-strain averaged curves for test data were plotted for all strain rates. The stress response in tension shows an increase in the yield and ultimate strengths and a general flattening of the subsequent softening as strain rate increases, which can be attributed to necking. The stress response in compression exhibits three regimes as noted in Fig. 4b: an initial linear elastic response followed by a nonlinear transition curve to global yield, followed by strain softening attributed to chain rearrangement and subsequent strain hardening attributed to the alignment of these chains.

3.3. Strain-life fatigue

Fig. 5 shows the strain-life curve for the polycarbonate at room temperature and at frequencies of 1 and 10 Hz. The curve exhibits

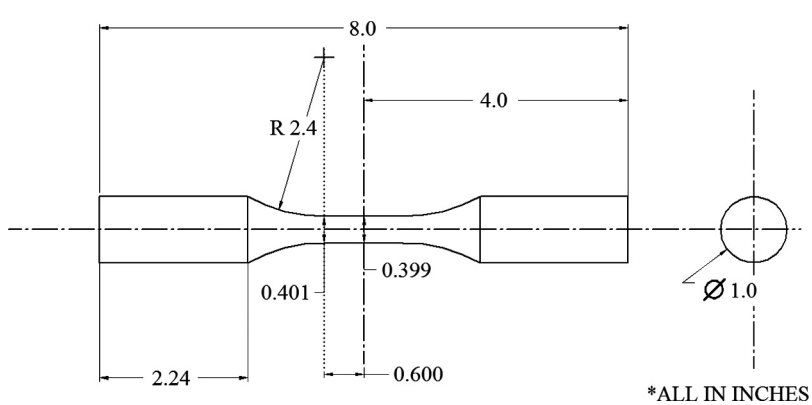

Fig. 1. Cylindrical dog-bone shaped specimens used for strain-life fatigue testing.

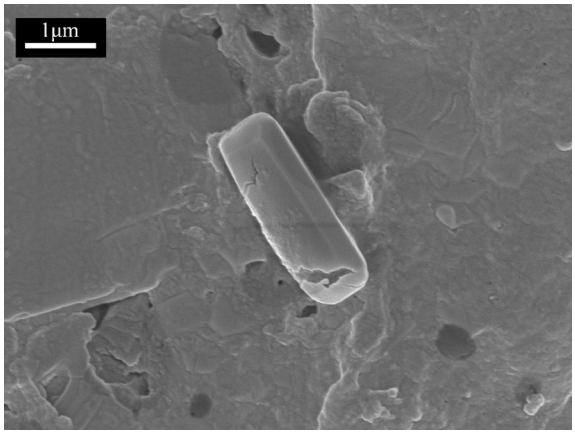

Fig. 2. Scanning Electron Microscope (SEM) image of a mostly intact polycarbonate pellet.

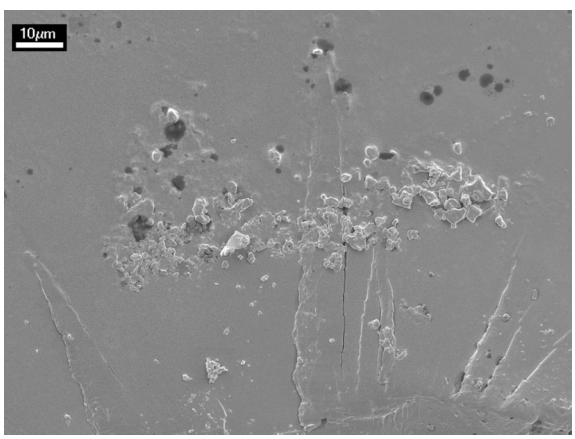

Fig. 3. Scanning Electron Microscope (SEM) image showing a conglomeration of particles which led to the nucleation of a dominant fatigue crack for a 0.0065 strain amplitude test at 10 Hz.

a plateau at lower strain amplitudes, previously defined as the long-life region by [23]. Before the plateau, a quasi linear section can be observed. While many thermoplastics exhibit frequency

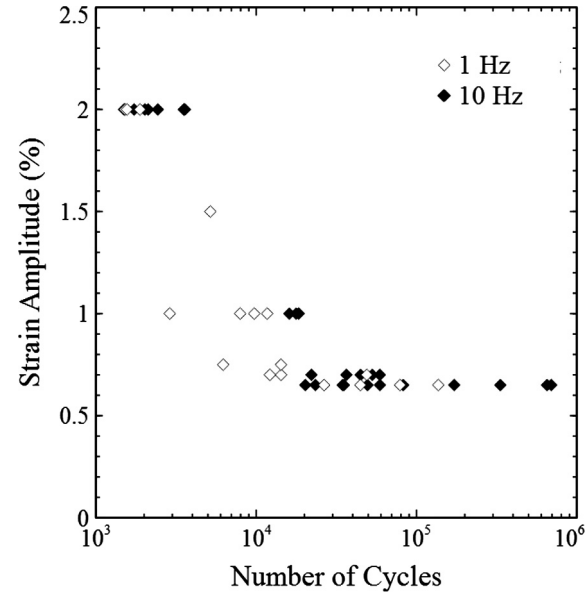

Fig. 5. Polycarbonate experimental strain-life fatigue plot for 1 and 10 Hz at room temperature.

dependent fatigue life curves, the PC of this study did not show this effect overall. Frequency effects have been studied previously (Hertzberg et al., 1975) where it was found that PC was particularly insensitive to test frequency, most likely due to a balance of competing strengthening and softening mechanisms, namely strain rate and creep effects.

3.4. Hysteresis stress response

Fig. 6 shows the initial and half-life hysteresis loops for the PC material indicating that a minimal energy dissipation occurred during cycling, resulting in a minimal hysteresis loop area and a near perfect overlap of the initial and mid-life hysteresis loops. This trend held true for all strain amplitudes and frequencies tested. Figs. 7a and b show the behavior of stress amplitude as a function of the number of cycles at strain amplitudes of 0.02 and 0.0065 at a frequency of 1 Hz, respectively. The stress amplitude

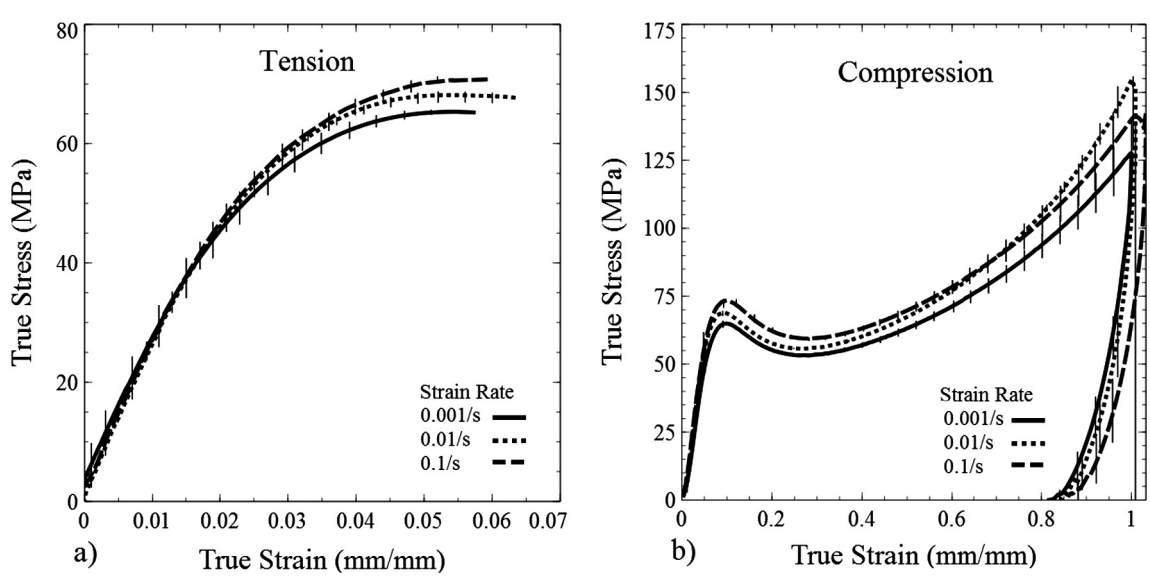

Fig. 4. Monotonic stress-strain plots of a Polycarbonate thermoplastic in (a) tension and (b) compression.

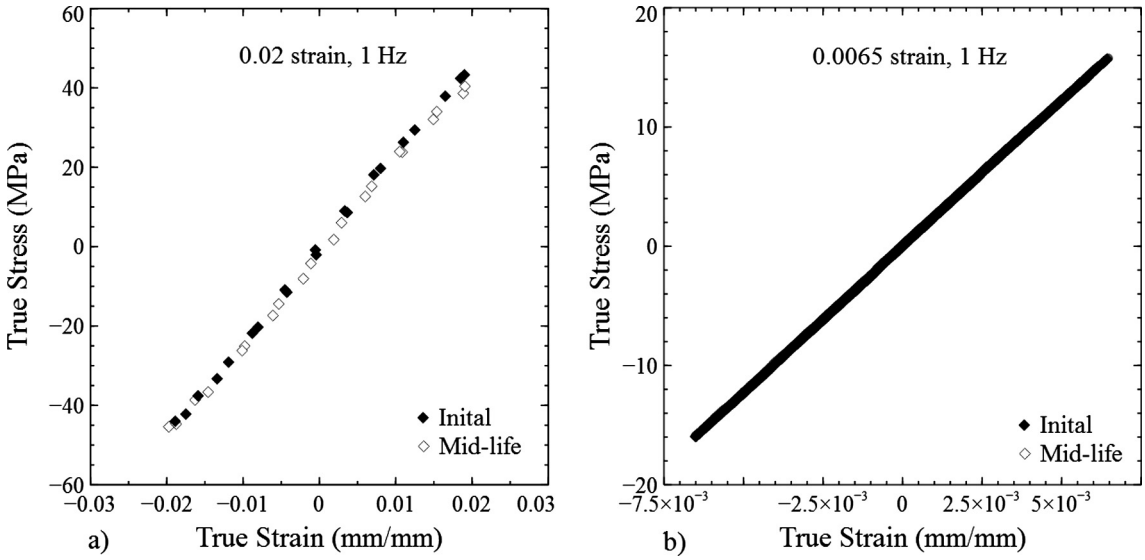

Fig. 6. Stress-strain hysteresis behavior for fatigue tests at 1 Hz for (a) 2% strain amplitude and (b) 0.65% strain amplitude.

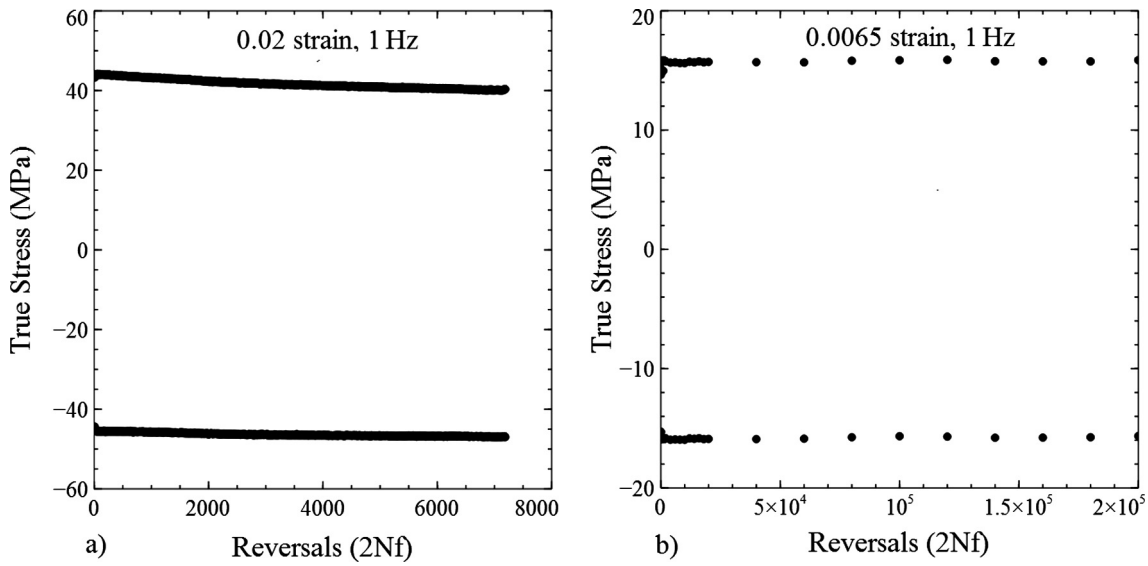

Fig. 7. Typical stress response versus reversals for (a) 0.02 strain amplitude test and (b) 0.0065 strain amplitude test.

is practically constant for all strain amplitudes tested. Only a minimal observable decay in the maximum tensile stress was observed at the higher strain amplitudes as shown in Fig. 7a.

3.5. Fractographic analysis

Fractography was performed on the fatigue fracture surfaces of the Polycarbonate copolymer specimens using Scanning Electron Microscopy (SEM) to characterize the fatigue damage in the material. Fig. 8 shows an overview of a fracture surface observed for PC showing the location of crack nucleation and the fatigue crack growth region. Fatigue damage marks can be observed as well as the different stages of damage regimes: incubation (INC), Microstructurally Small Crack (MSC), and long crack (LC). Adjacent to the incubation typical fatigue striations were observed with minimal craze formation at the crack tip.

Similar SEM micrographs to those shown in Fig. 8 have been observed previously [9,18]. Mackay et al. defined two zones: Zone 1 comprised the region where the crack initiated plus concentric marks around the crack initiation site, and Zone 2 identified by radial marks and some tangential striations. The striations observed in Zones 1 and 2 are typical of various thermoplastic materials like poly(vinyl chloride) [10], and polystyrene [26]. The concentric marks radiating from the failure origin in Zone 1 have been attributed to different stages of crack extension [9,18,10,26].

However, with the higher fidelity SEM equipment available today, better micrographs can be obtained. Fig. 8 shows an overall view of three distinct fatigue damage zones: an early crack growth stage with minimal craze formation at the crack tip (Fig. 9a) and a later crack growth stage with relatively large craze formations providing crack tip blunting and discontinuous crack growth (Fig. 9b). These three zones can be related to the established fatigue damage stages of the MultiStage Fatigue (MSF) model: crack incubation, MSC, and LC stages [29,19]. Since the fatigue striations marks of Fig. 9a are located immediately adjacent to the crack nucleation site, we assert that they belong to the MSC crack fatigue stage.

Similar to other studies using the MSF model [17,12,4], fatigue striations were correlated with MSC loading cycles. An example of

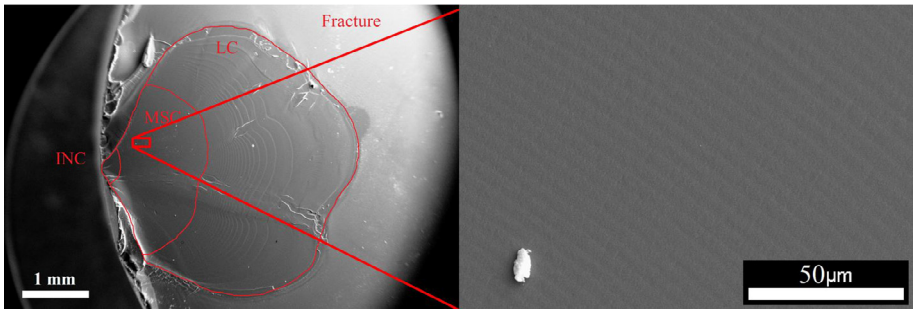

Fig. 8. Fatigue fracture surface of polycarbonate fatigue specimen showing three stages of fatigue damage: Inc: Incubation, MSC: small crack, and LC: Long crack.

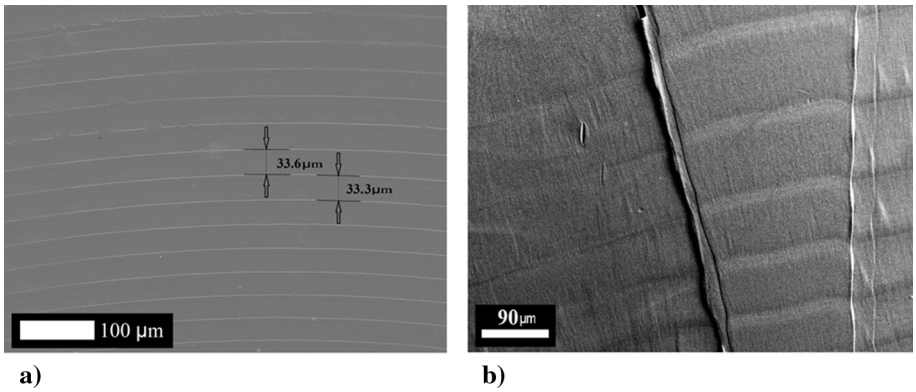

Fig. 9. (a) Fatigue striation width measurements for fatigue crack growth bands in polycarbonate and (b) discontinuous crack growth morphology formed during crack propagation on a specimen cycled at 2% strain amplitude at a frequency of 10 Hz showing crazed region ahead of crack arrest.

the striations is shown in Fig. 9a. Discontinuous crack growth morphology as observed via SEM imaging is shown in Fig. 9b. For these striations, a sub-band is clearly noticeable and is due to craze formation at the crack tip [9].

In addition, the SEM analysis revealed that cracks initiated at inclusion defects. The initiating defect size was quantified using the image analysis software ImageJ. For some specimens, there were no perceived crack incubating inclusions so it was assumed that these cracks incubated from crazes generated on the free surface of the specimens during cycling due to surface roughness. Fig. 10 shows the crack incubating inclusions for each specimen where an incubating inclusion could be found.

3.6. Fatigue crack growth

In the polymer community, a more complicated fatigue crack growth stage has been identified: discontinuous crack growth. In the discontinuous crack growth stage, a single striation does not necessarily correlate to a single load excursion, with the possibility of having hundreds to thousands of excursions before craze breakdown and crack extension as noted by *in-situ* studies [9] and can be attributed to crack tip stabilization by the craze formed at the crack tip. Despite the presence of discontinuous crack growth for some samples, striations were still measured, and in the case of clearly defined discontinuous crack growth bands striation length was taken from craze tip to craze tip. This effectively means that the crack growth curves will exclude discontinuous growth cycles by default. Within the context of the MSF model, discontinuous crack growth can be thought of as periods of crack incubation during intermittent periods of crack extension. For the current iteration of the plastics MSF model, the incubation regime will account for those cycles. Future model iterations will incorporate a discontinuous crack growth regime to separate the discontinuous crack growth and the crack incubation regimes for plastics.

Striation measurements were performed on fracture surfaces of the extremal failures (minimum and maximum life) fatigued at 0.0065 (Samples 1–4) and 0.02 (Samples 5 and 6) strain amplitude. Fig. 11 shows fatigue crack growth rates at 0.0065 and 0.02 strain amplitude for both 1 Hz and 10 Hz test frequencies. For both frequencies there is minimal observed dependency on test frequency, therefore, these results are in agreement with the statement that PC fatigue life is independent of test frequency as found by other researchers (3, 26).

4. Fatigue crack growth and modeling

4.1. Fatigue crack growth model

This study introduces a microstructure-sensitive small fatigue crack growth model based on crack tip displacements. [19] developed a fatigue model that decomposes the total fatigue life into three stages: incubation, small crack, and long crack as given by Eq. (1).

$$N_{Total} = N_{Inc} + N_{MSC} + N_{LC} \tag{1}$$

where N_{Total} is the total number of cycles, N_{Inc} is the number of cycles required to incubate a fatigue crack, N_{MSC} is the number of cycles spent in the microstructurally small/physically small crack (MSC) regime, and N_{LC} is the number of cycles of long crack (LC) growth until final failure. The transition between the MSC and LC regimes is governed by the crack growth rate. The crack growth rates for both the MSC and LC regimes are computed concurrently. When the crack growth rate for the LC regime exceeds that of the MSC regime, as long as material fracture has not occurred, the material exhibits LC growth. The LC regime for plastics has been studied extensively in the past [11,9,24,10], therefore this study only considers the small crack growth stage.

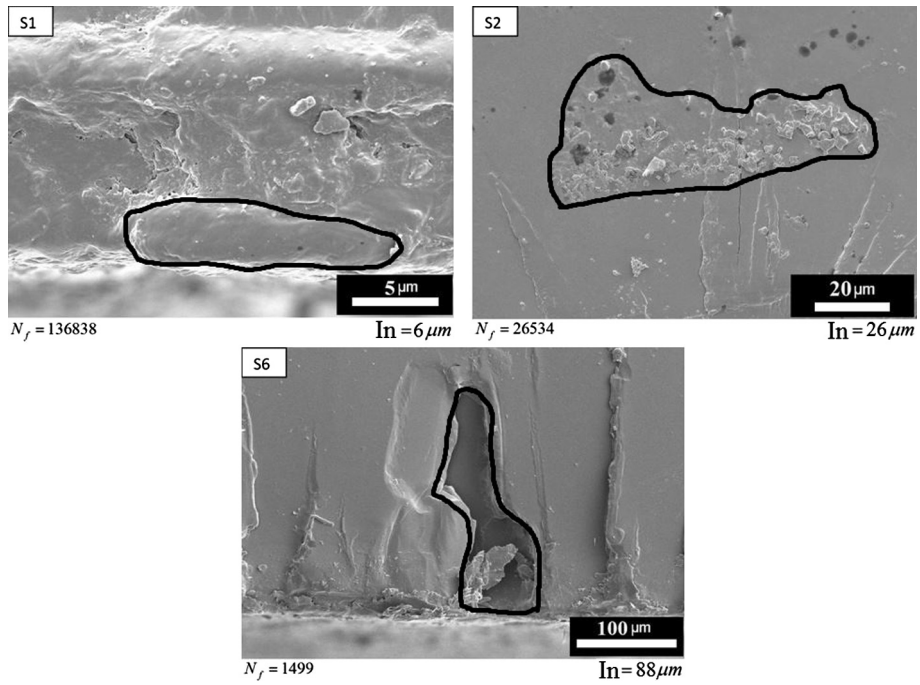

Fig. 10. Scanning Electron Micrograph (SEM) images of inclusions that nucleated fatigue cracks in selected samples where N_f is cycles to failure, and D is square root of the inclusion area.

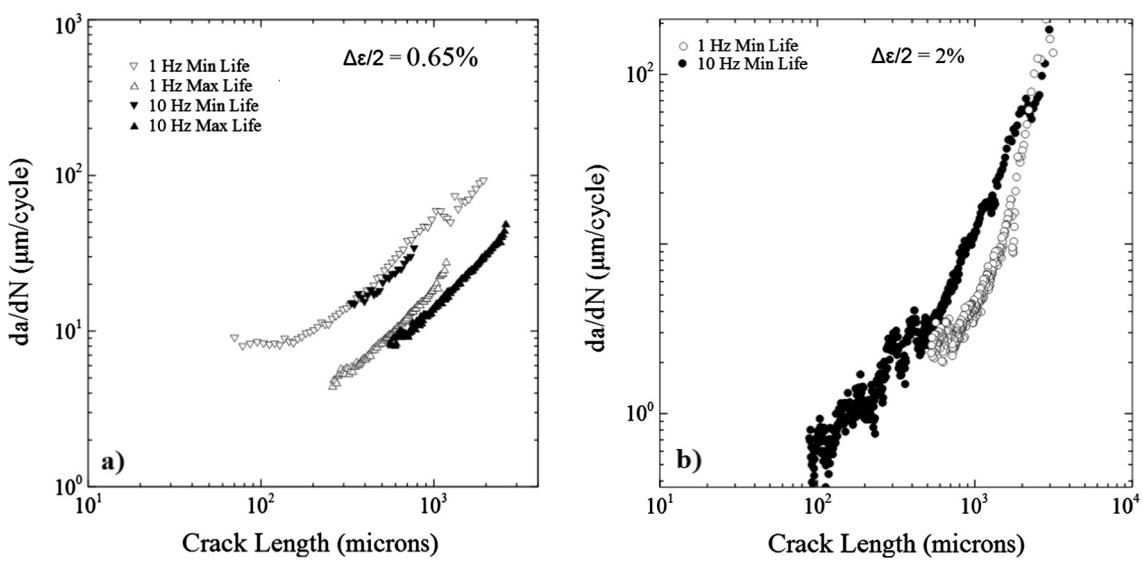

Fig. 11. Fatigue crack growth rates collected via striation measurements for polycarbonate for strain amplitudes of (a) 0.65% and (b) 2.0%.

The crack growth rate of the small fatigue crack regime (MSC) is a function of the crack tip displacement and is given by Eq. (2).

$$\frac{da}{dN} = \chi(\Delta CTD - \Delta CTD_{th}) \tag{2}$$

Where χ is a material dependent constant for a given microstructure typically less than unity [19] and ΔCTD_{th} is the crack tip displacement range threshold taken as the magnitude of the shear displacement of a sheared region of an amorphous polymer based on a dislocation analogue by [6].

The crack tip displacement range is related to the remote loading and is calculated by Eq. (3).

$$\Delta CTD = C_{II}\left(\frac{GS}{GS_0}\right)^{\zeta}\left(\frac{PS^2}{nnd * GS}\right)^{\xi}\left(\frac{U * \sigma * (1-R)}{S_{ult}}\right)^{m} a + C_I\left(\frac{GS}{GS_0}\right)^{\zeta}\left(\frac{PS^2}{nnd * GS}\right)^{\xi}\left(\frac{\Delta\gamma^p_{max}}{2}\right)^2 \tag{3}$$

$$\frac{\Delta\gamma^p_{max}}{2} = \frac{3}{2}\left(\frac{\sigma}{k'}\right)^{\frac{1}{n'}} \tag{4}$$

$$\varepsilon = \frac{\sigma}{E} + \left(\frac{\sigma}{k'}\right)^{\frac{1}{n'}} \tag{5}$$

Table 1
Polycarbonate microstructure and material properties for the fatigue crack growth model.

Property	Average	Standard deviation
Pore size (nm) [15]	0.595	0.030
Pore nearest neighbor (nm) [15]	0.83	0.04
Young's modulus (MPa)	2490	240
Ultimate strength (MPa)	68.18	0.44

Table 2
PC MSC model calibration parameters.

Property	Average	Standard deviation
k'	110	5.5
n'	0.18	0.008
CTDth (μm) [6]	0.000425	0.000021
CI	0	0
CII	1000	0
χ [19]	0.32	0
m	−3.039	0
ξ	1.277	0
ζ	2.022	0
GS_0	16	0

The first term of Eq. (3) accounts for small crack growth under high cycle fatigue (HCF) while the second term incorporates the low cycle fatigue (LCF) effects. The term

$$\left(\frac{PS^2}{nnd * GS}\right)$$

represents the effect of pore size distribution on small crack growth (MSC). *PS* is the size of the distributed pores in the polymer matrix, *nnd* is the nearest neighbor distance between pores, GS is the grain size for a given metal, and GS_0 is a normalizing factor. Generally, the GS term is used as a normalization factor for the pore size effects and is typically the next largest microstructural scale. For the PC material, the incubating inclusion size ("size" column of Table 1) is used as this normalization factor due to the lack of significant microstructural details for an amorphous polymer. The term σ is the remote applied cyclic stress calculated from the Ramberg-Osgood relationship (5) using a Newton-Raphson method. The parameter *U* is employed to incorporate the strain ratio effects and is defined as

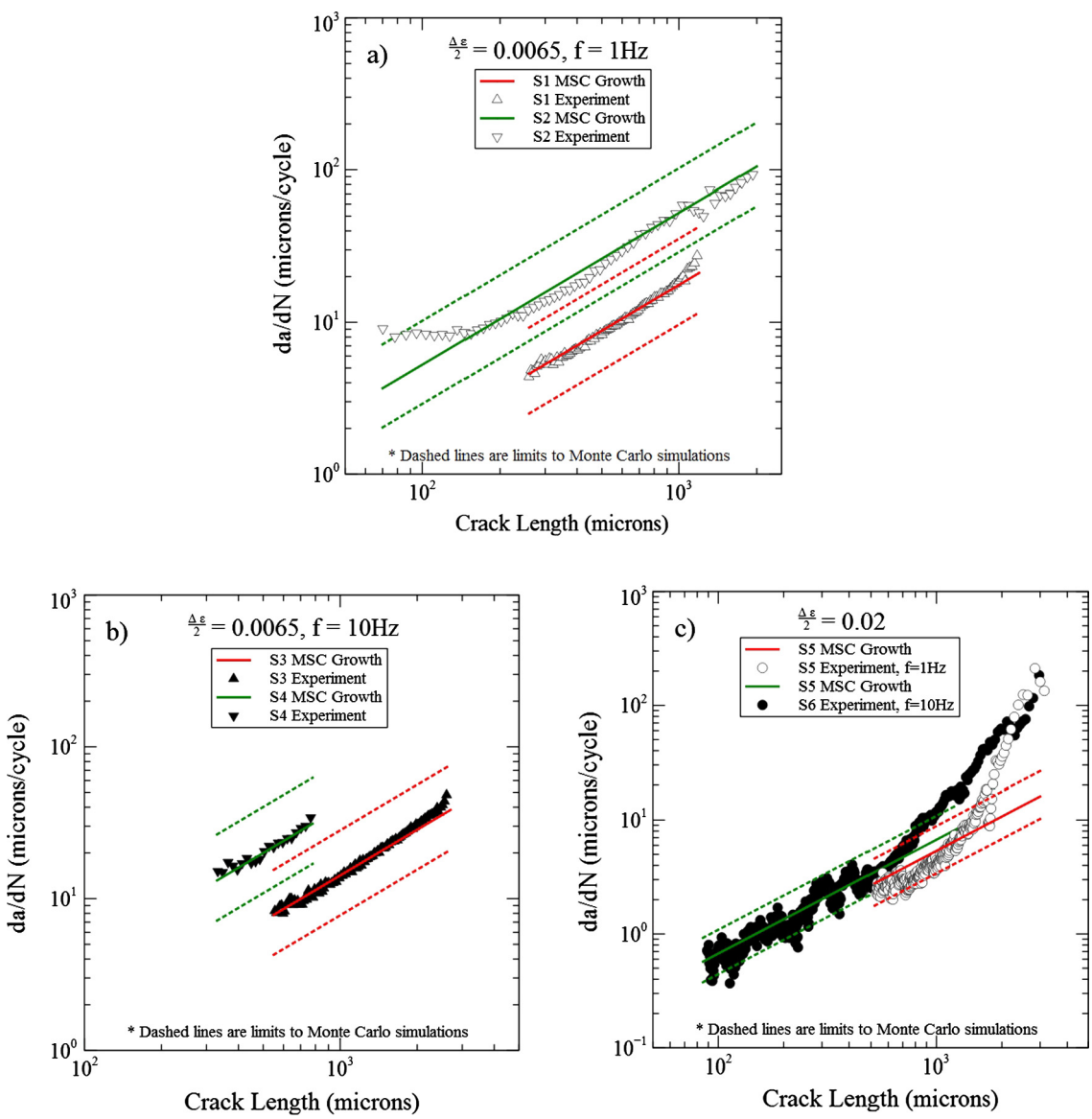

Fig. 12. MSC model correlations and uncertainty bounds of each selected test sample for (a) a strain amplitude of 0.0065 and frequency of 1 Hz, (b) a strain amplitude of 0.0065 and frequency of 10 Hz, and (c) a strain amplitude of 0.02 at frequencies of 1 and 10 Hz.

$$U = \frac{1}{1 - R}$$

for R values less than zero and as U = 1 for R values of zero and greater where R is applied load ratio (27). Finally,

$$\frac{\Delta\gamma^{p}_{\max}}{2}$$

is the remote maximum applied plastic shear strain range where k' and n' are the cyclic strength coefficient and cyclic strain hardening exponent, respectively, from the Ramberg-Osgood relationship.

4.2. Small fatigue crack growth modeling correlations

Distributed porosity will affect fatigue crack growth. Voids on the order of two to five angstroms in diameter have been observed by Bohlen [5] using Positron Annihilation Lifetime Spectroscopy (PALS) for a similar material subjected to varying temperature and pressure. Kristiak and Bartos [15] has published a summary of PC microstructural features and are shown in Table 1. In the computations of the MSF model, these values for the microstructure were employed and a single parameter set was found to describe all experimental data.

To assess model uncertainty, a Monte Carlo (MC) simple random sampling routine was used to propagate each parameter's statistical distribution through the model. Due to having sparse data, normal distributions are assumed. Table 2 gives the model parameters resulting from the calibration to the samples of known incubating inclusion size, and where applicable, the calculated standard deviations. Only experimental parameters are considered in the uncertainty quantification method. For the parameters gathered from references, the standard deviation was assumed to be five percent of the average as a conservative estimate. The strain measurements from the extensometer are precise to 0.5% of the strain reading in accordance to ASTM E83 [2].

It is important to note that since this model was originally created using multiscale calculations pertinent to the physics of metals, the current implementation is incapable of directly assessing the effects of polymer specific modes of deformation and crack growth (crazing, chain slippage, chain entanglement, etc.). Therefore, the current implementation for plastics takes on a semi-empirical role. An important fatigue crack growth mechanism present in polymers, crack tip blunting and stress relaxation due to crazing, is not present in this model. This is evident in the model's calibration with the stress effect exponent. Since local stress relaxation is not taken into account, the current implementation of the model has an inverse relationship with remote applied stress; that is, higher remote applied stresses lead to lower crack growth rates. This same trend is evident in the crack growth rate curves for each remote applied strain. Though counter intuitive with respect to normal fatigue crack growth with metals, it is believed that the negative exponent artificially accounts for the effects of crazing on crack growth. This may be corrected by future polymer small crack growth research including the effects of crazing and crack tip blunting.

Fig. 12 shows the model calibration compared to each experimental crack growth curve. Overall, the MSC model correlates well with the experimental data by only changing the incubating inclusion size. For Fig. 12a and b, the crack growth rate curves follow a typical log-linear increase in growth rate [9]. For the higher applied strains of Fig. 12c, the crack growth rate curves exhibit a sudden increase and is most likely due to a transition to the long crack regime. The jagged nature of the 0.02 applied strain crack growth curves are most likely due to the crack front overcoming barriers along its path. The log-linear sections of each experimental crack growth curve falls within the uncertainty bands for its respective model correlation with minimal overlap of uncertainty ranges between curves for samples with disparate incubating inclusion sizes. This shows that the current model calibration is capable of distinguishing between each crack incubation condition (i.e. inclusion size dependency) for materials that do not exhibit test frequency dependency. For materials whose fatigue lives are highly frequency dependent, modification of the model is necessary to capture the effects of test frequency on the peak cyclic stresses and material properties.

5. Conclusions

Fatigue crack growth rates and microstructure properties were quantified via SEM imaging and input into the MSF microstructurally small crack growth model for calibration. The following conclusions are a result of this study.

(1) This model is an implementation of the metals model from [19]. It is important to note that the current implementation is incapable of directly assessing the effects of polymer specific modes of deformation and crack growth.
(2) The current iteration of the model is shown to be general enough to capture the behavior of fatigue crack growth in a frequency independent, amorphous polycarbonate thermoplastic. Future work will need to incorporate the effects of test frequency on material properties along with their subsequent effect on the peak cyclic stress.
(3) Though the incubation regime can be used to account for discontinuous growth cycles, it is only intended for tracking the cycles before a crack has begun. Due to the existence of discontinuous crack growth, a new regime is required to separate the phenomenon.
(4) A single parameter set can be used to describe all possible crack growth rates by changing only the incubating inclusion size. The model is capable of distinguishing between different crack growth curves with differing incubating inclusion sizes. This is supported by the minimal overlap of model uncertainty bands for samples with disparate inclusion sizes.
(5) For small crack growth, microstructural features ahead of the crack front such as particles would affect crack growth rates. However, for this iteration of the model calibration routine, particle sizes ahead of the crack tip are not taken into account directly within the model framework. Future work needs to include the effects of particle size and distribution ahead of the crack tip and their subsequent effect on stress evolution by using finite element modeling.
(6) The model does not take into account polymer specific modes of deformation such as crazing and shear banding. Typically, crazing produces a line of voids spanned by groups of polymer chains ahead of the crack tip and serves to blunt the crack tip and reduce the cyclic stress. Modification of the remote applied stress or using local stress approximations subject to the effects of polymer crazing to account for stress relaxation ahead of the crack front will lead to better model correlations.

Acknowledgments

This material is based upon work supported by the U.S. Army TACOM Life Cycle Command under contract No. 256HZV-08-C-0236, through a subcontract with Mississippi State University, and was performed for the Simulation Based Reliability and Safety (SimBRS) research program. Reference herein to any specific com-

mercial company, product, process, or service by trade name, trademark, manufacturer, or otherwise, does not necessarily constitute or imply its endorsement recommendation, or favor by the United States government or the Department of the Army (DoA). The opinions of the authors expressed herein do not necessarily state or reflect those of the United States government or the DoA and shall not be used for advertising or product endorsement purposes. The authors would also like to thank the Center for Advanced Vehicular Systems (CAVS) at Mississippi State University.

References

[1] ASTM Standard D412. Vol. 09.01, rubber, natural and synthetic – general test methods, carbon black. ASTM International; 2008.
[2] ASTM Standard E83. Vol. 10, standard practice for verification and classification of extensometer systems. ASTM International; 2016.
[3] Bannantine JA, Comer JJ, Handrock JL. Fundamentals of metal fatigue analysis. Prentice Hall; 1990.
[4] Bernard JD, Jordon JB, Lugo M, Hughes JM, Rayborn DC, Horstemeyer MF. Observations and modeling of the small fatigue crack behavior of an extruded AZ61 magnesium alloy. Int J Fatigue 2013;52:20–9.
[5] Bohlen J, Kirchheim R. Macroscopic volume changes versus changes in free volume as determined by positron annihilation lifetime spectroscopy for polycarbonate and polystyrene. Macromolecules 2001;34:4210–5.
[6] Bowden PB, Raha S. A molecular model for yield and flow in amorphous glassy polymers making use of a dislocation analogue. Philos Mag 1974;29:149.
[7] Bureau MN, Dickson JI, Denault J. Comparison of the fatigue propagation behaviour of Polystyrene and 95/5 Polystyrene/polyethylene blends. J Mater Sci 1998;33:1591–606.
[8] Elinck JP, Bauwens JC, Homes G. Fatigue crack growth in poly(vinyl chloride). Int J Fract Mech 1971;7(3):277–87.
[9] Hertzberg RW, Manson JA. Fatigue of engineering plastics. New York: Academic Press; 1980.
[10] Hertzberg RW, Manson JA. Micromechanisms of fatigue-crack advance in PVC. J Mater Sci 1973;8(11):1554–8.
[11] Hertzberg RW, Nordberg H, Manson JA. Fatigue crack propagation in polymeric materials. J Mater Sci 1970;5(6):521–6.
[12] Jordon JB, Bernard JD, Newman JC. Quantifying microstructurally small fatigue crack growth in an aluminum alloy using a silicon-rubber replica method. Int J Fatigue 2012;36(1):206–10.
[13] Kim HS, Wang XM. Temperature and frequency effects on fatigue crack growth in acrylonitrile-butadiene-styrene (ABS). J Appl Polym Sci 1995;57(7):811–7.
[14] Konczol L, Doll W, Bevan L. Mechanisms and micromechanics of fatigue crack propagation in glassy thermoplastics. Colloid Polym Sci 1990;268:814–22.
[15] Kristiak J, Bartos J. Free-volume microstructure of amorphous polycarbonate at low temperatures determined by positron-annihilation-lifetime-spectroscopy. Am Phys Soc 1994;49(10):6601–7.
[16] Lowe A, Kwon O-H, Mai Y-W. Fatigue and fracture behaviour of novel rubber modified epoxy resins. Polymer 1996;37(4):565–72.
[17] Lugo Marcos, Fountain Jason E, Hughes Justin M, Bouvard Jean-Luc, Horstemeyer MF. Microstructure-based fatigue modeling of an acrylonitrile butadiene styrene (ABS) copolymer. J Appl Polym Sci 2014;131(20).
[18] Mackay ME, Teng T-G, Schultz JM. Craze roles in the fatigue of polycarbonate. J Mater Sci 1979;14:221–7.
[19] McDowell DL, Gall K, Horstemeyer MF, Fan J. Microstructure-based fatigue modeling of cast A356–T6 alloy. Eng Fract Mech 2003;70:49–80.
[20] Mulliken AD, Boyce MC. Mechanics of the rate-dependent elastic-plastic deformation of glassy polymers from low to high strain rates. Int J Solids Struct 2006;43:1331–56.
[21] Newman JC, Wu XR, Swain MH, Zhao W, Phillips EP, Ding CF. Small-crack growth and fatigue life predictions for high-strength aluminium alloys. Part II: Crack closure and fatigue analyses. Fatigue Fract Eng Mater Struct 2000;23(1):59–72.
[22] Niinomi M, Wang L, Enjitsu T, Fukanaga K-I. Fatigue characteristics of ultra high molecular weight polyethylene with different molecular weight. J Mater Sci: Mater Med 2001;12:267–72.
[23] Rabinowitz S, Krause AR, Beardmore P. Failure of polystyrene in tensile and cyclic deformation. J Mater Sci 1973;8:11–22.
[24] Radon JC. Fatigue crack growth in polymers. Int J Fract 1980;16(6):533–52.
[25] Schinker MG, Konczol L, Doll W. Micromechanics of fatigue crack propagation in glassy thermoplastics. Colloid Polym Sci 1984;262:230–5.
[26] Skibo MD, Hertzberg RW, Manson JA. Fatigue fracture processes in polystyrene. J Mater Sci 1976;11(3):479–90.
[27] Skibo MD, Hertzberg RW, Manson JA, Kim SL. On the generality of discontinuous fatigue crack growth in glassy polymers. J Mater Sci 1977;12(3):531–42.
[28] Stephens RI, Fatemi A, Stephens RR, Fucks HO. Metal fatigue in engineering. 2nd ed. Wiley-Interscience; 2000.
[29] Suresh S. Fatigue of materials. 2nd ed. United Kingdom: Cambridge University Press; 1998.
[30] Suresh S, Ritchie RO. Propagation of short cracks. Int Met Rev 1984;29(6):445–76.
[31] Wu XR, Newman JC, Zhao W, Swain MH, Ding CF, Phillips EP. Small-crack growth and fatigue life predictions for high-strength aluminium alloys. Part I: Experimental and fracture mechanics analysis. Fatigue Fract Eng Mater Struct 1998;21(1):1289–306.
[32] Xue YA, McDowell DL, Horstemeyer MF, Dale MH, Jordan JB. Microstructure-based multistage fatigue modeling of aluminum alloy 7075–T651. Eng Fract Mech 2007;74:2810–23.
[33] Xue YA, Horstemeyer MF, McDowell DL, El-Kadiri H, Fan J. Microstructure-based multistage fatigue modeling of a cast AE44 Magnesium Alloy 2007b;29:666–76.